

Article

Ribes nigrum Leaf Extract Preferentially Inhibits IFN- γ -Mediated Inflammation in HaCaT Keratinocytes

Andrea Magnavacca ^{1,†} , Stefano Piazza ^{1,†} , Anna Cammisia ², Marco Fumagalli ¹, Giulia Martinelli ¹ , Flavio Giavarini ¹, Enrico Sangiovanni ^{1,*}  and Mario Dell'Agli ¹ 

¹ Department of Pharmacological and Molecular Sciences, University of Milan, 20133 Milan, Italy; andrea.magnavacca@unimi.it (A.M.); stefano.piazza@unimi.it (S.P.); marco.fumagalli3@unimi.it (M.F.); giulia.martinelli@unimi.it (G.M.); flavio.giavarini@unimi.it (F.G.); mario.dellaghi@unimi.it (M.D.)

² Specialist in Dermatology and Venereology, Corso di Porta Romana 131, 20122 Milan, Italy; acammisa.doc@gmail.com

* Correspondence: enrico.sangiovanni@unimi.it

† Contributed equally to this work.

Abstract: *Ribes nigrum* L. (blackcurrant) leaf extracts, due to high levels of flavonols and anthocyanins, have been shown to exhibit beneficial effects in inflammatory diseases. However, whereas their traditional use has been investigated and validated in several models of inflammation and oxidative stress, the possible impact on skin disorders is still largely unknown. The purpose of this work was to elucidate the effects of *R. nigrum* leaf extract (RNLE) on keratinocyte-derived inflammatory mediators, elicited by a Th1 or Th2 cytokine milieu. HaCaT cells were challenged with TNF- α , either alone or in combination with the costimulatory cytokines IFN- γ or IL-4, and the release of proinflammatory cytokines and mediators (IL-8, IL-6, s-ICAM-1, and TSLP) was evaluated. The results showed that RNLE preferentially interferes with IFN- γ signaling, demonstrating only negligible activity on TNF- α or IL-4. This effect was attributed to flavonols, which might also account for the ability of RNLE to impair TNF- α /IL-4-induced TSLP release in a cAMP-independent manner. These results suggest that RNLE could have an antiallergic effect mediated in keratinocytes via mechanisms beyond histamine involvement. In conclusion, the discovery of RNLE preferential activity against IFN- γ -mediated inflammation suggests potential selectivity against Th1 type response and the possible use in Th1 inflammatory diseases.

Keywords: *Ribes nigrum*; blackcurrant leaves; skin; inflammation; keratinocytes; IFN- γ ; TSLP



Citation: Magnavacca, A.; Piazza, S.; Cammisia, A.; Fumagalli, M.; Martinelli, G.; Giavarini, F.; Sangiovanni, E.; Dell'Agli, M. *Ribes nigrum* Leaf Extract Preferentially Inhibits IFN- γ -Mediated Inflammation in HaCaT Keratinocytes. *Molecules* **2021**, *26*, 3044. <https://doi.org/10.3390/molecules26103044>

Academic Editors: María De La Luz Cádiz-Gurrea, Antonio Segura-Carretero and David Arráez-Román

Received: 24 April 2021

Accepted: 17 May 2021

Published: 20 May 2021

Publisher's Note: MDPI stays neutral with regard to jurisdictional claims in published maps and institutional affiliations.



Copyright: © 2021 by the authors. Licensee MDPI, Basel, Switzerland. This article is an open access article distributed under the terms and conditions of the Creative Commons Attribution (CC BY) license (<https://creativecommons.org/licenses/by/4.0/>).

1. Introduction

Ribes nigrum L. (blackcurrant) is a deciduous shrub belonging to the family Grossulariaceae and native to the temperate regions of the northern hemisphere. A number of scientific papers have shown the beneficial effects of blackcurrant in inflammatory diseases due to high levels of anthocyanins and proanthocyanidins [1]. Herbal teas made with blackcurrant leaves have traditionally been used to relieve urinary complaints and minor articular pain [2]. Accordingly, the oral administration of the dried leaves, standardized to the flavonoid content (>1.5%, expressed as rutin), has been reported by the ESCOP monographs as adjuvant in the treatment of rheumatic conditions [3]. The main flavonoids occurring in blackcurrant leaves belong to the class of flavonols, of which the most mentioned are quercetin and kaempferol glycosides [4]. In addition, proanthocyanidins and phenolic acids may occur as well [5].

The traditional use of blackcurrant leaf extracts rich in polyphenols has been investigated and validated in various models of inflammation [6,7] and oxidative stress [8]; however, the possible impact on skin disorders is still largely unknown. Recently, our research group extensively reviewed the preclinical data on the effect of *Ribes* spp. At the skin level [1]; an ointment containing 1% methanolic *R. nigrum* leaf extract showed

wound-healing properties in vivo [8], while the oral administration of a quercitrin-rich hydroalcoholic extract of *Ribes fasciculatum* Maxim. roots attenuated the allergic response in a mouse model of atopic dermatitis (AD) [9].

According to the latest scientific advances, the role played by keratinocytes in the pathogenesis of inflammatory-based skin diseases is crucial. Keratinocytes directly interface with the external environment, taking part in the barrier homeostasis and communicating with the resident immune system. The alteration of these structural and regulatory functions is associated with common skin diseases such as psoriasis and AD (for excellent reviews on the topic, see Kim et al. [10] and Girolomoni et al. [11]). An antimicrobial peptide (cathelicidin or LL-37), released from injured keratinocytes, was recently recognized as the antigen triggering the autoimmune response occurring in psoriatic patients (Th1-mediated), which is characterized by elevated levels of IFN- γ produced by Th1/Th17 lymphocytes [12]. Similarly, cytokines released by damaged epidermis, such as thymic stromal lymphopoietin (TSLP) and IL-33, may trigger the pruritogenic and humoral response in AD patients (Th2-mediated), mediated by elevated levels of IL-4, IgE, and histamine (see the review by Corren and Ziegler [13]). Notably, psoriasis and AD are commonly referred to as prototypes of Th1 and Th2 inflammatory diseases, respectively. Nevertheless, mediators from both types of inflammatory response are involved in their pathogenesis.

Several in vitro studies have elucidated, at least in part, the way in which keratinocytes may respond to innate immunity (TNF- α , IL-1 β), as well as Th1 (e.g., IFN- γ , IL-17) and Th2 (e.g., IL-4) cytokines. Firstly, they are able to amplify the inflammatory process in response to innate immunity cytokines, through the expression of chemokines (e.g., CCL-2, CCL-20, CXCL-8/IL-8, and CXCL10), cytokines (e.g., IL-1 β , TNF- α , IL-6, and IL-17C) [14,15], and surface proteins (e.g., ICAM-1, MHC) [16,17], in order to recruit different classes of leukocytes. In this context, the transcription factor NF- κ B plays a fundamental role; in fact, it is involved in the expression of all the aforementioned classes of proinflammatory mediators.

Moreover, keratinocytes may release a relevant number of cytokines in response to the adaptive immune response. For example, different authors have shown that IL-6 production is elevated by IL-4 or IFN- γ in keratinocytes, especially in a histamine-enriched milieu [18,19]; IL-6 may play a dual role in autoimmunity by contributing to the humoral response through the polarization of Th2 and B lymphocytes [20] and promoting Th1/Th17 differentiation [21]. In analogy, Kim et al. [22] conducted excellent work in optimizing a cytokine milieu able to reproduce AD-like inflammation in a model of human keratinocytes (HaCaT). In this cell line, the expression of AD-related biomarkers requires induction with cytokines characteristic of both the innate (TNF- α) and the adaptive (IL-4, IFN- γ) immune responses, thus remarking the complexity of the pathogenesis at the keratinocyte level. In fact, the combination of TNF- α with IFN- γ is required to enhance IL-33 expression, while the combination of TNF- α with IL-4 is necessary to enhance TSLP expression. Notably, both combinations cause a parallel decrease in several indicators of epidermal integrity and differentiation.

As of today, the role of *R. nigrum* leaf extracts against keratinocyte-derived inflammation is still unrevealed. According to recent reviews on the topic, the contribution of flavonols to the biological properties of blackcurrant leaves has only marginally been evaluated by previous authors [23]. The purpose of this work was to investigate the effects of an aqueous extract of *Ribes nigrum* L. leaves in a model of human keratinocytes (HaCaT) challenged with TNF- α , either alone or in combination with the costimulatory cytokines IFN- γ (5 ng/mL) or IL-4 (100 ng/mL). The experimental setting aimed at mimicking Th1 or Th2 type responses, respectively. Following this approach, the preferential activity of the extract against IFN- γ -mediated inflammation was discovered, thus suggesting a potential selectivity against Th1 response.

2. Results

2.1. Phytochemical Analysis

Ribes nigrum leaf extract (RNLE), a dry extract obtained from the aqueous extraction of *Ribes nigrum* L. leaves, was subjected to a phytochemical analysis aimed at identifying the main phenolic compounds, with particular attention paid to flavonoids.

The total phenolic content (TPC) was initially assessed by Folin–Ciocâlțeu assay, which displayed a value (mean \pm SD) of 17.260 ± 0.473 mg/g_(extract), expressed as gallic acid equivalents.

Quantitative analysis of the extract by LC–MS/MS showed the presence of several flavonoids, especially quercetin and kaempferol derivatives. The percentage of identified phenolic compounds was 13.8%; the occurrence of individual flavonoids/phenolics is reported in Table 1.

Table 1. Quantitative analysis of phenolic compounds occurring in RNLE.

Compound	Molecular Weight (<i>m/z</i> of [M – H] ^{−1})	Retention Time (min)	wt.% in RNLE
Kaempferol aglycone	285	9.06	2.9%
Kaempferol-7-glucoside	447	7.53	3.8%
Kaempferol-3-glucoside	447	7.48	1.3%
Quercetin aglycone	301	8.52	1.9%
Hyperoside	463	7.26	0.8%
Rutin	610	7.09	1.6%
Chlorogenic acid	353	6.68	1.5%

2.2. RNLE Increases *IL-10* Expression in *TNF- α* -Induced HaCaT Cells

The therapeutic relevance of *TNF- α* -signaling inhibition in skin inflammation has been highlighted by the clinical efficacy of anti-*TNF- α* drugs (i.e., etanercept). Consequently, applying a comprehensive approach, the effect of RNLE (100 μ g/mL) on *TNF- α* -challenged HaCaT cells was first evaluated in a multigenic qPCR macroarray.

In line with our previous study [14], *TNF- α* caused the overexpression of genes involved in monocyte and granulocyte recruitment (*CCL2*, *CCL7*, *CSF2*, *CXCL5*, *CXCL1*), as well as in lymphocyte chemoattraction and activation (*CXCL11*, *IL6*) (Figures 1 and 2). RNLE was able to partially revert the upregulation of *CCL7*, *CSF2*, *CXCL1*, and *CXCL11*, although this effect did not reach statistical significance (Figures 2 and 3). It is worth considering that these genes are target of the transcription factor NF- κ B [24]. The most peculiar finding was that the strongest inhibitory trend was observed for *CXCL11*, a gene encoding an IFN- γ -inducible chemokine, regulated, similarly to *CXCL10* and *ICAM-1*, by NF- κ B and STAT-1 activity [25]. In addition, *TNF- α* also caused a slight downregulation of the anti-inflammatory *IL10* gene, while the concomitant treatment with RNLE resulted in a significant induction of *IL10* expression (Figure 4), thus suggesting a possible pro-resolving mechanism. However, the overexpression of *IL10* mRNA was not paralleled by an increment in *IL-10* protein levels, whether in the intracellular compartments or those secreted in the culture medium (data not shown).

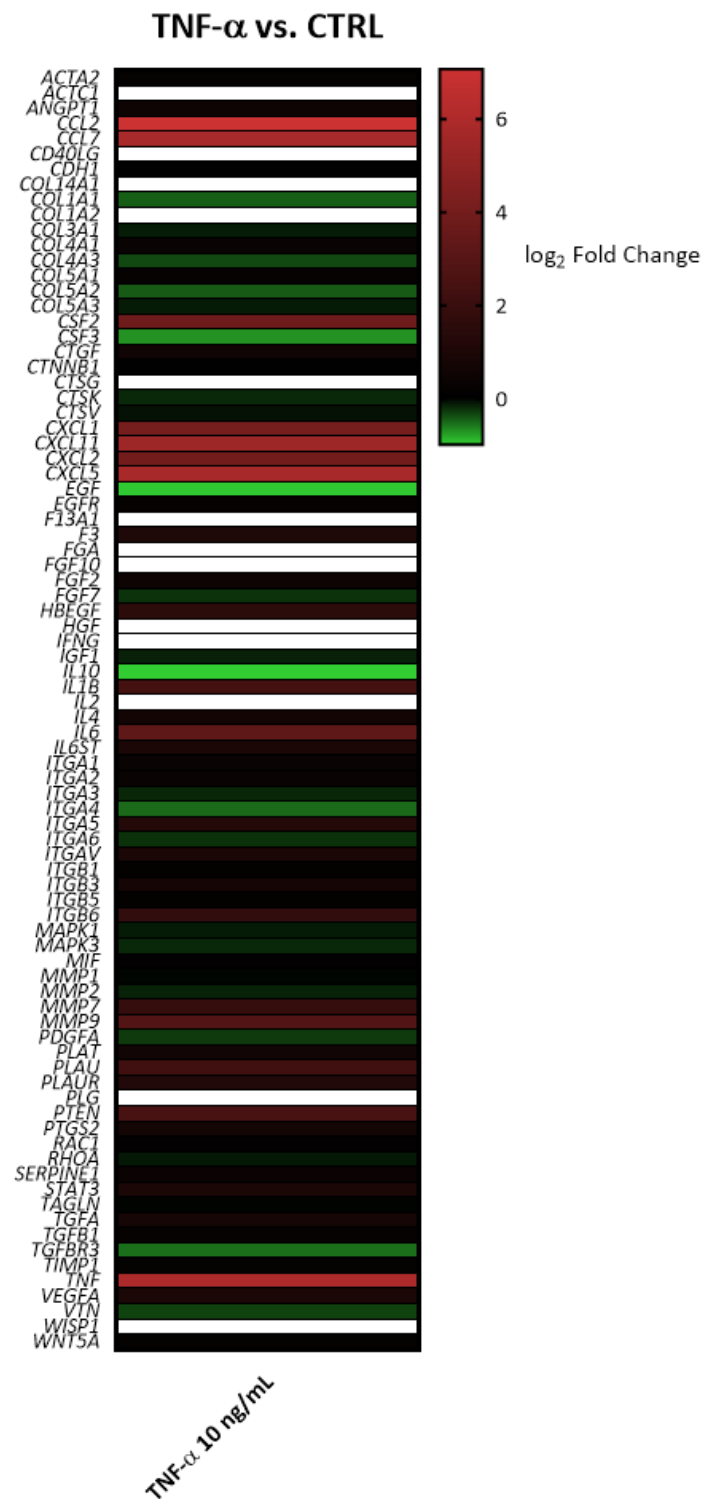


Figure 1. Heatmap depicting the alterations of gene expression induced by TNF- α (10 ng/mL, 6 h). The color scale represents gene upregulation (**red**) and downregulation (**green**) compared to the control (\log_2 fold change = 0, **black**). In white, genes present in the panel but not expressed in the experimental model.

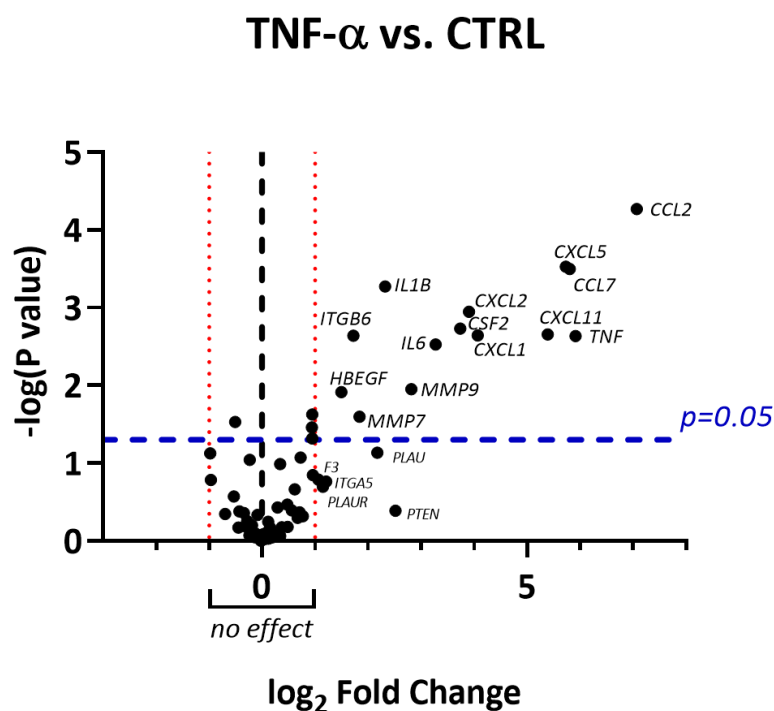


Figure 2. Volcano plot showing the entity of gene up/downregulation induced by TNF- α (10 ng/mL, 6 h) together with statistical significance. Only genes with absolute fold change greater than 2 (\log_2 fold change greater than 1) and $p < 0.05$ were considered significantly regulated.

2.3. RNLE Inhibits TNF- α /IFN- γ - but Not TNF- α -Induced IL-8 Release in HaCaT Cells

The previous results, regarding gene expression, suggested that RNLE may cover a marginal role against a TNF- α -induced inflammatory profile. However, TNF- α is known to synergize with IFN- γ to enhance a classical Th1 response in keratinocytes, triggering a wider program for pathogen clearance. In particular, IFN- γ is frequently used to prime cells for a stronger response toward TNF- α during *in vitro* experiments. At a molecular level, the activation of the JAK/STAT-1 pathway by IFN- γ cooperates with the transcriptional activity of NF- κ B during TNF- α -induction; thus, the combination of TNF- α and IFN- γ has been shown to strongly induce the expression of IL-8, IL-6, and ICAM-1, considered to be among the most relevant proinflammatory mediators in keratinocytes [26,27].

As a consequence, we performed a series of experiments aimed at assessing the effect of RNLE (25–100 μ g/mL) on the synergic contribution of IFN- γ in TNF- α -challenged HaCaT cells. RNLE inhibited IL-8 release following stimulation with a combination of both cytokines, but not when TNF- α was used alone (Figure 5).

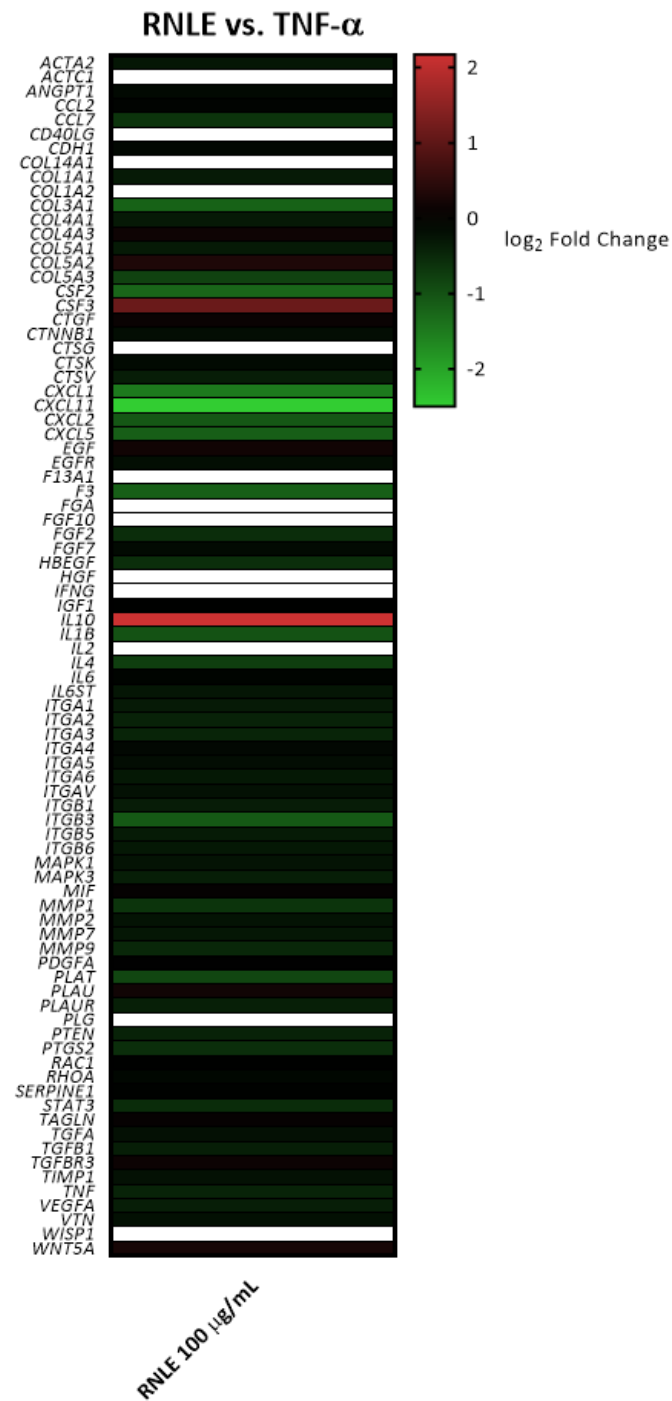


Figure 3. Heatmap depicting the effect on gene expression induced by RNLE treatment (100 µg/mL) in HaCaT cells stimulated with TNF- α (10 ng/mL, 6 h). The color scale represents gene upregulation (red) and downregulation (green) compared to TNF- α -induced condition (log₂ fold change = 0, black). In white, genes present in the panel but not expressed in the experimental model.

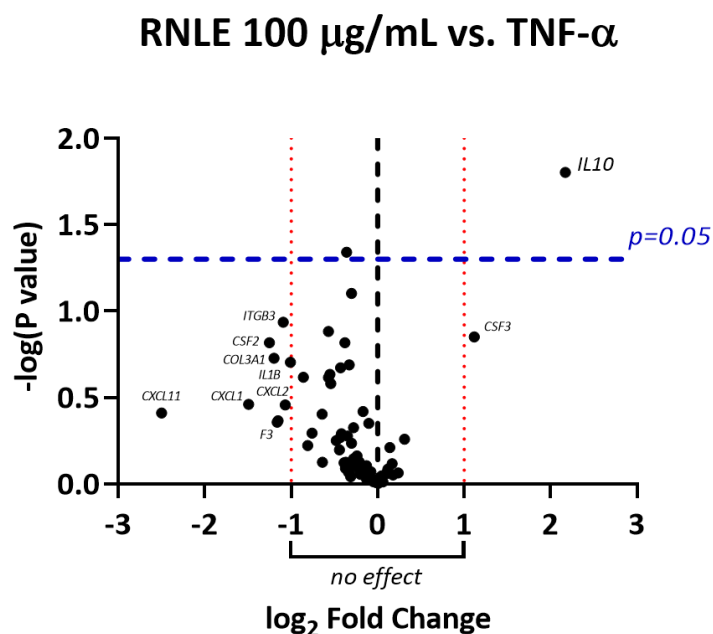


Figure 4. Volcano plot showing the entity of gene up/downregulation induced by RNLE treatment (100 µg/mL) in HaCaT cells stimulated with TNF- α (10 ng/mL, 6 h) together with statistical significance. Only genes with absolute fold change greater than 2 (\log_2 fold change greater than 1) and $p < 0.05$ were considered significantly regulated.

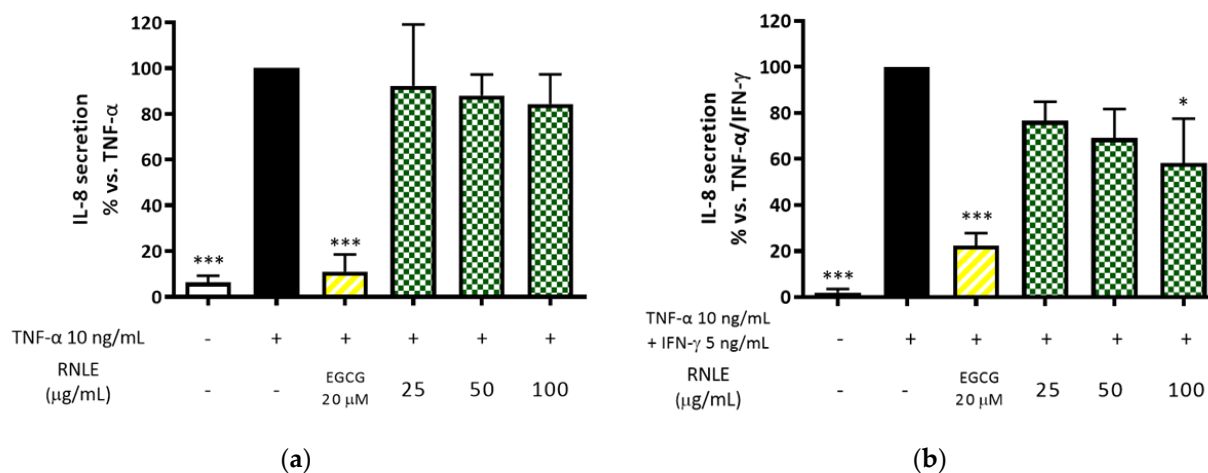


Figure 5. (a) Effect of RNLE treatment (25–100 µg/mL) on IL-8 secretion in HaCaT cells stimulated with TNF- α (10 ng/mL, 24 h); the amount of IL-8 in the stimulated condition was 211.31 ± 34.26 pg/mL. (b) Effect of RNLE treatment (25–100 µg/mL) on IL-8 secretion in HaCaT cells stimulated with a combination of IFN- γ and TNF- α (5 ng/mL + 10 ng/mL, 24 h); the amount of IL-8 in the stimulated condition was 1084.66 ± 118.62 pg/mL. (–) Epigallocatechin 3-gallate (EGCG) 20 µM was used as the reference compound; * $p < 0.05$, *** $p < 0.001$ vs. stimulus.

In line with the inhibitory trend observed for *CXCL11* expression, this experiment suggests that RNLE may preferentially interfere with IFN- γ , rather than TNF- α , signaling.

2.4. RNLE Inhibits TNF- α /IFN- γ -Induced IL-6 Release in HaCaT Cells

Accordingly, we evaluated the effect of RNLE on the release of IL-6 in TNF α /IFN- γ -challenged HaCaT cells. Notably, preliminary time-course experiments (Figure A3, Appendix A) showed that IFN- γ (5 ng/mL) was necessary for a considerable induction of IL-6 release (149.52 ± 35.48 pg/mL) by TNF- α (10 ng/mL), which could not be achieved (35.67 ± 9.73 pg/mL) by TNF- α alone. On the other hand, IFN- γ alone was not sufficient to induce the release of the cytokine, thus reflecting its priming role in the response to

TNF- α in this experimental setting. In this sense, the regulation of IL-6 release displays a marked difference if compared to IL-8, for which TNF- α by itself is sufficient to obtain a considerable induction.

RNLE (25–50 $\mu\text{g}/\text{mL}$) totally abrogated IL-6 release (Figure 6). In line with the experimental setting, the suppression of IFN- γ signaling would have accounted for a stronger inhibitory effect on IL-6 rather than IL-8 release. Consequently, these results reinforced the hypothesis of a preferential activity of RNLE against IFN- γ signaling.

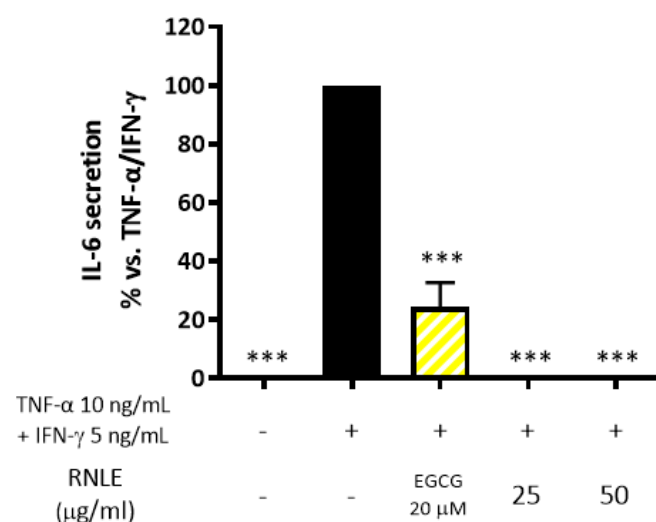


Figure 6. Effect of RNLE treatment (25–50 $\mu\text{g}/\text{mL}$) on IL-6 secretion in HaCaT cells stimulated with a combination of IFN- γ and TNF- α (5 ng/mL + 10 ng/mL, 24 h); the amount of IL-6 in the stimulated condition was 118.66 ± 15.95 pg/mL. (–)-Epigallocatechin 3-gallate (EGCG) 20 μM was used as the reference compound; *** $p < 0.001$ vs. stimulus.

2.5. RNLE Preferentially Inhibits IFN- γ - over TNF- α -Induced s-ICAM-1 Release in HaCaT Cells

ICAM-1 is a cell-surface adhesion molecule which allows the interaction between cells and leukocytes at the site of inflammation. Its soluble form (s-ICAM-1) is produced after cleavage and represents a well-established marker of cellular activation, strongly correlated with the induction of ICAM-1 expression [28]. As previously demonstrated in the scientific literature, ICAM-1 is induced by TNF- α and IFN- γ in many cellular types including keratinocytes [16,29]. Notably, IFN- γ was reported to elicit ICAM-1 expression at lower concentration than TNF- α in HaCaT cells [17]. In our experiments, we could observe an analogous behavior, since a concentration of IFN- γ half that of TNF- α led to a similar quantitative release of s-ICAM-1 (422.97 ± 90.28 and 512.99 ± 84.17 pg/mL for IFN- γ and TNF- α , respectively).

RNLE (25–50 $\mu\text{g}/\text{mL}$) inhibited both TNF- α - and IFN- γ -induced s-ICAM-1 release. Nevertheless, this effect was displayed in a concentration-dependent fashion with a preferential impairment of IFN- γ versus TNF- α challenge (Figure 7), thus confirming our previous observations. The vascular protective activity of the flavonols present in RNLE, including the inhibition of adhesion molecules, is well known [30,31]. To the best of our knowledge, the bioactivity of flavonols against ICAM-1 expression has been less investigated in keratinocytes than in other cellular populations. Bitto et al. showed that quercetin and taxifolin counteract IFN- γ -induced ICAM-1 expression in keratinocytes, thus suggesting the potential involvement of flavonols in RNLE activity [32].

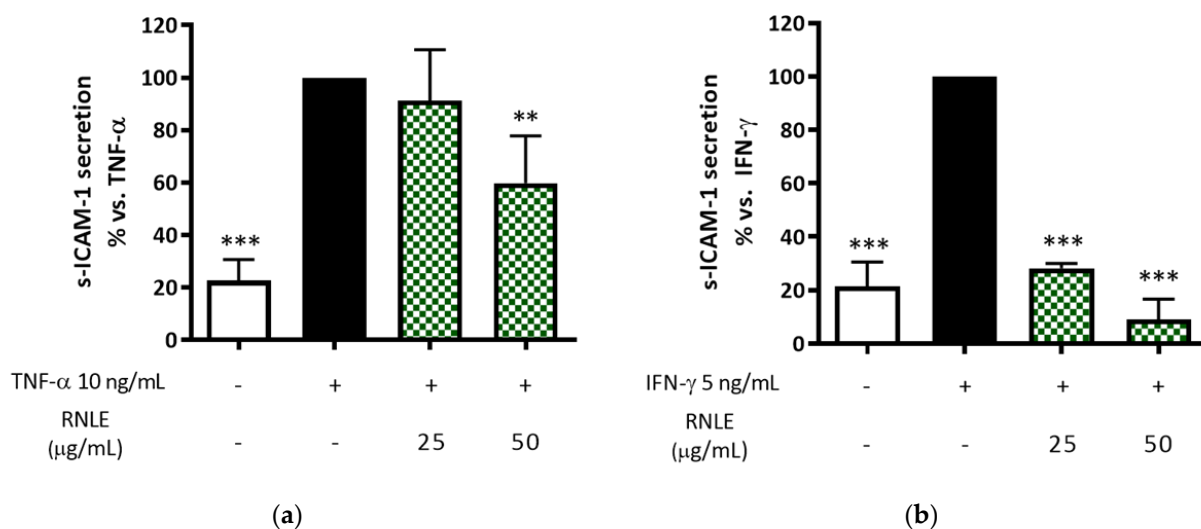


Figure 7. (a) Effect of RNLE treatment (25–50 µg/mL) on s-ICAM-1 secretion in HaCaT cells stimulated with TNF-α (10 ng/mL, 24 h); the amount of s-ICAM in the stimulated condition was 512.99 ± 84.17 pg/mL. (b) Effect of RNLE treatment (25–50 µg/mL) on s-ICAM-1 secretion in HaCaT cells stimulated with IFN-γ (5 ng/mL, 24 h); the amount of s-ICAM in the stimulated condition was 422.97 ± 90.28 . ** $p < 0.01$, *** $p < 0.001$ vs. stimulus.

2.6. RNLE Inhibits TNF-α/IFN-γ-Induced NF-κB Activity in HaCaT Cells

As previously mentioned, NF-κB plays a pivotal role in the promoter activity of IL-8, IL-6, and ICAM-1. Consequently, in the subsequent experiments, we wondered whether an interference in this mechanism might account for the activity of RNLE. Following the previous approach, HaCaT cells were treated with RNLE concomitantly with TNF-α or TNF-α/IFN-γ stimulation.

In line with the aforementioned inhibition of IFN-γ-induced inflammatory markers, the activity of NF-κB was impaired by a concentration of RNLE as low as 25 µg/mL under TNF-α/IFN-γ stimulation; on the contrary, the extract was unable to counteract NF-κB activity under TNF-α stimulation (Figure 8). This evidence demonstrates that RNLE may counteract IFN-γ signaling at least at a transcriptional level, thus arousing interest in the use of blackcurrant leaves against Th1 inflammation in skin.

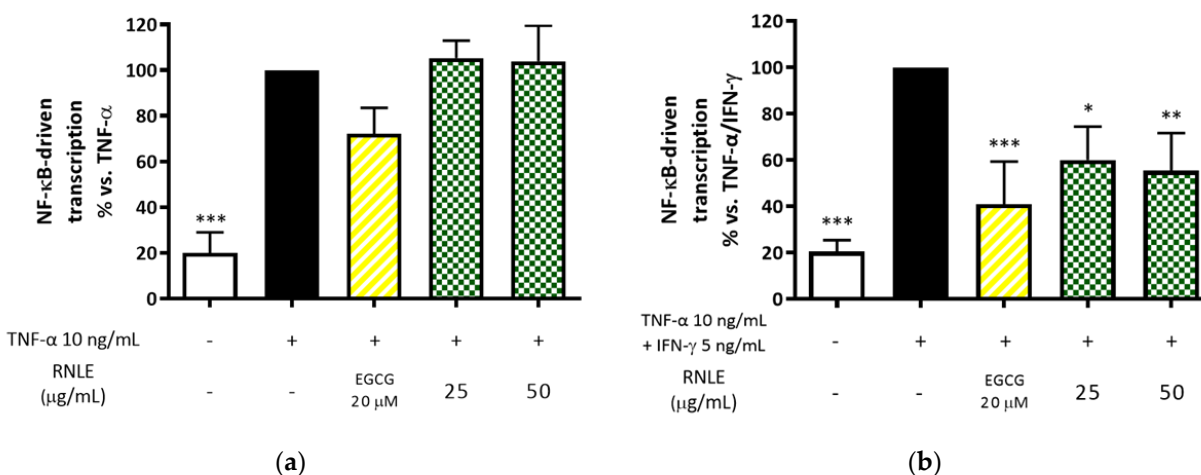


Figure 8. (a) Effect of RNLE treatment (25–50 µg/mL) on NF-κB-driven transcription in HaCaT cells stimulated with TNF-α (10 ng/mL, 24 h). (b) Effect of RNLE treatment (25–100 µg/mL) on NF-κB-driven transcription in HaCaT cells stimulated with a combination of IFN-γ and TNF-α (5 ng/mL + 10 ng/mL, 24 h). (–) Epigallocatechin 3-gallate (EGCG) 20 µM was used as the reference compound; * $p < 0.05$, ** $p < 0.01$, *** $p < 0.001$ vs. stimulus.

2.7. RNLE Is Not Able to Inhibit TNF- α /IL-4-Induced IL-6 Release in Differentiated HaCaT Cells

At this point of the work, we decided to shift our focus to the initial question regarding the possible selectivity of RNLE against Th1 or Th2 type responses in keratinocytes. At first, we observed that RNLE was able to enhance mRNA but not protein levels of IL-10, a widely recognized pro-resolving type 2 mediator. Then, after having found that IFN- γ -inducible mediators were conversely impaired by the extract, we moved to the investigation of the bioactivity against TNF- α /IL-4 stimulation as a model of Th2 inflammation.

In the last few years, the scientific research has elucidated the ways in which inflammation and differentiation are interweaved in keratinocytes. According to the literature, IL-6 not only plays a critical role in the differentiation of the lymphocyte sub-population involved in skin autoimmunity [10], but also acts on keratinocytes by impairing their differentiation [33]. In fact, IL-6 and IL-4 were shown to downregulate markers of early (keratin-1, keratin-10) and terminal (involucrin) differentiation [34,35]. Consequently, we selected IL-6 release as a suitable outcome for either the investigation of RNLE activity against TNF- α /IL-4 stimulation and the dissection of the role of RNLE in Th1 or Th2 response.

For this purpose, we differentiated HaCaT cells by maintaining HaCaT cells under validated cultural conditions [34,36] and then verified the effect of TNF- α /IL-4 stimulation on IL-6 release during the differentiation time (from 3 to 11 days). IL-4 enhanced the effect of TNF- α on IL-6 release, and their synergy was magnified with the progression of differentiation. Notably, in this context, TNF- α alone was sufficient to induce IL-6 release, but secreted levels (224.60 ± 47.02 pg/mL) did not increase over the differentiation period (Figure A4, Appendix A). Although the involvement of IL-4 in the alteration of the epidermal barrier has been elucidated, studies regarding the role of differentiation in the response to IL-4 in keratinocytes were not extensive. We did not further investigate the molecular machinery behind the contribution of the differentiation to the effect of IL-4; however, Nishio et al. [37] demonstrated that proteins downstream of IL-4 receptor (JAK2/STAT-6) are more expressed in the granular layer of the healthy skin than in the lower layers. Differentiated HaCaT cells are referred to as a model of early differentiation; thus, theoretically, the increase in JAK2/STAT-6 expression during differentiation is plausible and may enhance the IL-4 response.

Consequently, we evaluated the effect of RNLE on differentiated cells, stimulated by the combination of TNF- α and IL-4. In contrast to previous observations, RNLE (25–50 μ g/mL) was unable to significantly impair IL-6 release in this experimental setting (Figure 9). The result suggested a marginal impact of RNLE on IL-4 signaling.

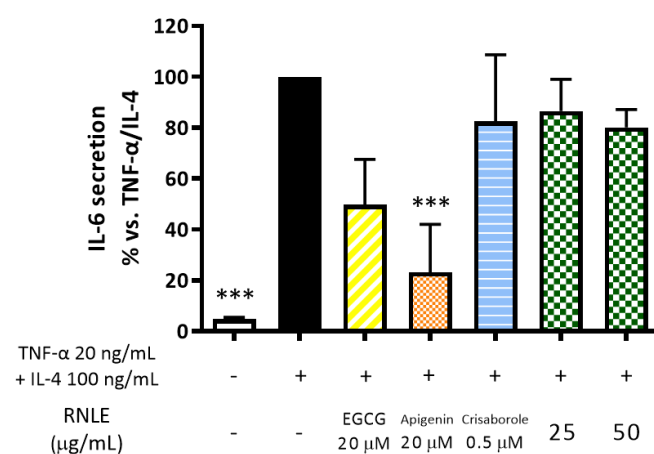


Figure 9. Effect of RNLE treatment (25–50 μ g/mL) on IL-6 secretion in differentiated HaCaT cells stimulated with a combination of IL-4 and TNF- α (100 ng/mL + 20 ng/mL, 24 h); the absolute amount of IL-6 in the stimulated condition was 612.59 ± 59.55 pg/mL. (–)–Epigallocatechin 3-gallate (EGCG) 20 μ M, apigenin 20 μ M, and crisaborole 0.5 μ M were used as the reference compounds; *** $p < 0.001$ vs. stimulus.

2.8. RNLE Inhibits TNF- α /IL-4-Induced TSLP Release in Differentiated HaCaT Cells with a cAMP-Independent Mechanism

To more deeply evaluate the actual role of RNLE in Th2 response, we selected the cytokine TSLP, i.e., another type 2 cytokine involved in atopic inflammation through the activation of dendritic and ILC2 cells, as an additional outcome [13]. In AD and psoriatic patients, TSLP has been shown to preferentially accumulate in the upper layers of the epidermis and, among skin cells, originates exclusively from keratinocytes [22,38]. Moreover, in analogy with IL-6, its levels correlate with the impairment of epidermal integrity [39].

According to our experiments, TSLP was released (65.05 ± 31.91 pg/mL) by HaCaT cells only late in the differentiation period and required the combination of TNF- α and IL-4. This result was concordant with the experiments conducted on inflamed human skin explants by Bogiatzi et al. [38], in terms of the amount of TSLP release and the prerequisite of differentiation for this effect to be observed.

Consequently, the effect of RNLE on TSLP was evaluated in differentiated HaCaT cells stimulated with the combination TNF- α /IL-4, under the same experimental setting applied for the investigation of IL-6 release. In these conditions, RNLE inhibited TSLP release by 56% at a concentration of 50 μ g/mL (Figure 10).

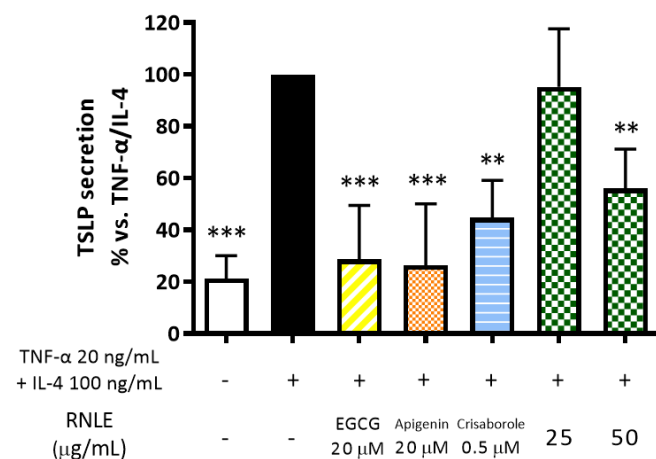


Figure 10. Effect of RNLE treatment (25–50 μ g/mL) on TSLP secretion in differentiated HaCaT cells stimulated with a combination of IL-4 and TNF- α (100 ng/mL + 20 ng/mL, 24 h); the absolute amount of TSLP in the stimulated condition was 65.05 ± 31.91 pg/mL. (–)–Epigallocatechin 3-gallate (EGCG) 20 μ M, apigenin 20 μ M, and crisaborole 0.5 μ M were used as the reference compounds; ** $p < 0.01$, *** $p < 0.001$ vs. stimulus.

The molecular machinery responsible for TSLP release by keratinocytes is not completely clear, but NF- κ B and NFAT may play an important role in TSLP transcription in response to mechanical and biological injuries [40,41].

The pharmacological inhibition of PDE4 and the elevation of intracellular cAMP levels were demonstrated to impair the proinflammatory activity of transcription factors (such as NFAT and NF- κ B), leading to the inhibition of cytokine production, including TSLP [42,43]. Moreover, cAMP elevation was associated with keratinocyte differentiation [44]. Notably, many flavonoids are well-known NF- κ B inhibitors and also possess inhibitory activity on different PDE isoforms, including PDE4 [45,46]. Among them, the flavone apigenin was shown, on the one hand, to non-selectively inhibit PDE4 [47] and, on the other, to reduce the levels of proallergic cytokines in models of asthma and atopic dermatitis [48,49]; however, a causal link between the two effects could not be established. For these reasons, we decided to further correlate the effect of RNLE with that of crisaborole (0.5 μ M), a topical PDE4 inhibitor approved in 2016 by FDA for the treatment of AD. Apigenin (20 μ M) was included in the experiments as a representative flavonoid.

Since crisaborole and apigenin exhibited a strong inhibitory effect on TSLP release (Figure 8), we speculated that the bioactivity of RNLE might involve a cAMP-dependent mechanism. Consequently, we measured intracellular cAMP levels in the same experimental setting. Apigenin and crisaborole, as expected, caused an increase in intracellular cAMP levels, whereas RNLE could not induce this molecular mechanism (Figure 11). However, EGCG (20 μ M), used as a positive control in each experiment, showed the ability to impair TSLP release in the absence of cAMP elevation, thus suggesting that RNLE may act through cAMP-independent mechanisms as well.

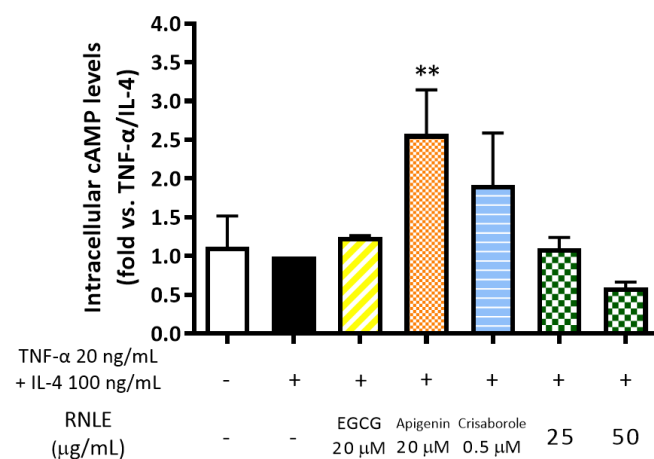


Figure 11. Effect of RNLE treatment (25–50 μ g/mL) on intracellular cAMP levels in differentiated HaCaT cells stimulated with a combination of IL-4 and TNF- α (100 ng/mL + 20 ng/mL, 24 h). (–) Epigallocatechin 3-gallate (EGCG) 20 μ M, apigenin 20 μ M, and crisaborole 0.5 μ M were used as the reference compounds; ** $p < 0.01$ vs. stimulus.

2.9. RNLE Slightly Inhibits TNF- α /IL-4-Induced NF- κ B Activity in HaCaT Cells

NF- κ B has been demonstrated to regulate both TSLP and IL-6 expression. However, TSLP and IL-6 release was differently modulated by RNLE treatment in our experiments; thus, we decided to investigate the effect of the extract on NF- κ B activation to better clarify its involvement. In line with the substantial absence of an inhibitory effect on IL-6 release and the lack of cAMP-elevating activity, RNLE was not able to counteract TNF- α /IL-4-induced NF- κ B-driven transcription, although a slight but not statistically significant inhibition was observed at 50 μ g/mL (Figure 12).

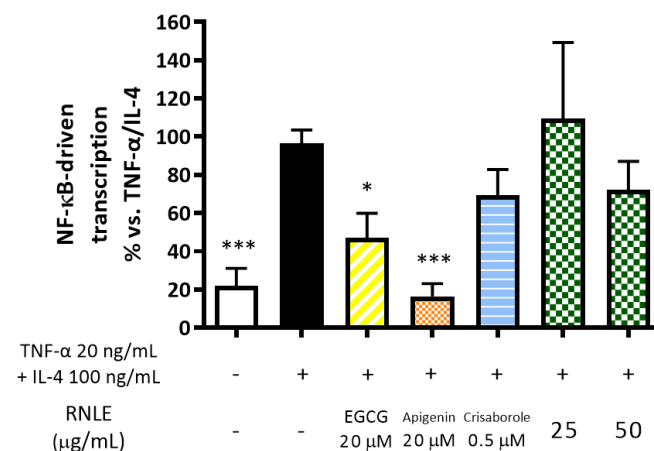


Figure 12. Effect of RNLE treatment (25–50 μ g/mL) on NF- κ B-driven transcription in HaCaT cells stimulated with a combination of IL-4 and TNF- α (100 ng/mL + 20 ng/mL, 6 h). (–) Epigallocatechin 3-gallate (EGCG) 20 μ M, apigenin 20 μ M, and crisaborole 0.5 μ M were used as the reference compounds; * $p < 0.05$, *** $p < 0.001$ vs. stimulus.

It is intriguing to note that RNLE at a concentration of 50 $\mu\text{g}/\text{mL}$ paralleled the effect of crisaborole (0.5 μM) with regard to all TNF- α /IL-4-related parameters (IL-6, TSLP, NF- κB -driven transcription), with the exception of cAMP levels. This observation suggests that the effect of RNLE on TSLP release might not be due directly to cAMP levels, but rather to the cAMP-independent activity on downstream cAMP-dependent proteins and cAMP sensors with anti-inflammatory implications, such as PKA and EPAC (see the reviews by Murray [50] and Woo and Kuzel [51]). In line with this hypothesis, several authors have demonstrated that flavonols may activate PKA- and EPAC-dependent pathways [52,53]. Notably, the activation of PKA/CREB signaling may also contribute to the overexpression of IL-10 [54], as previously observed, thus reinforcing the hypothesis that the activity of the extract under study might be potentially due to flavonols.

2.10. RNLE Is Not Able to Inhibit Histamine-Induced IL-6 Release in HaCaT Cells

TSLP involved is involved in not only Th2 cell maturation but also itch elicitation. Its action is either direct on sensory neurons [55] or indirect through dendritic, ILC2, and mast-cell stimulation [13]. Histamine is a key mediator of itch and allergic inflammation, which has been shown to enhance the release of several cytokines by inflamed keratinocytes, including TSLP and IL-6 [18,19].

In line with the findings of Wölflé et al. [56], we verified that IL-6 release is effectively induced by the combination of histamine (100 μM) and TNF- α in HaCaT cells. Consequently, we assessed if RNLE might also counteract the signaling of histamine, by selecting IL-6 as the experimental outcome. As shown in Figure 13, RNLE was unable to inhibit histamine alone or histamine/TNF- α -stimulated IL-6 secretion in comparison with cetirizine (0.1 μM).

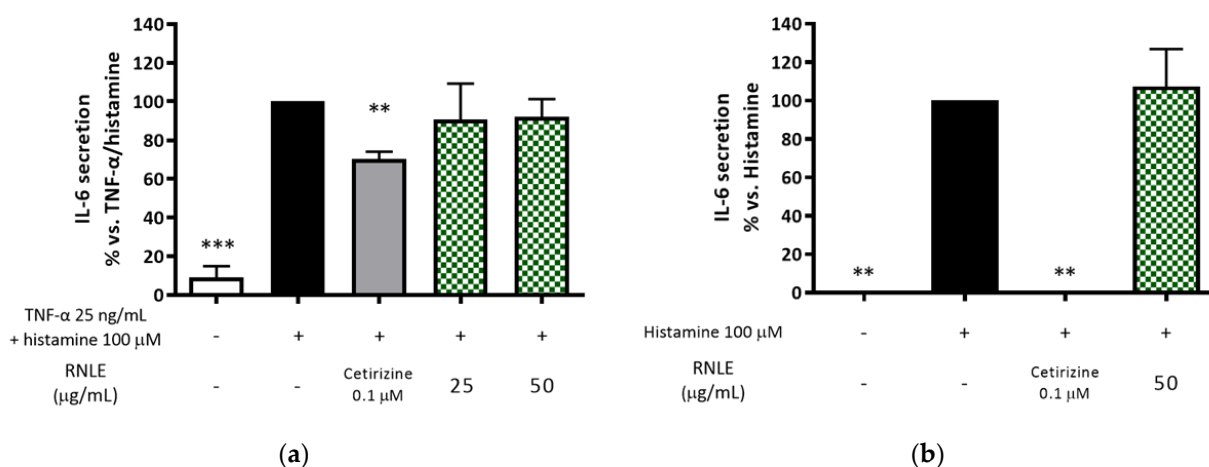


Figure 13. (a) Effect of RNLE treatment (25–50 $\mu\text{g}/\text{mL}$) on IL-6 secretion in HaCaT cells stimulated with a combination of histamine and TNF- α (100 μM + 25 ng/mL, 24 h); the amount of IL-6 in the stimulated condition was 64.50 ± 25.85 pg/mL. (b) Effect of RNLE treatment (25–50 $\mu\text{g}/\text{mL}$) on IL-6 secretion in HaCaT cells stimulated with histamine (100 μM , 24 h); the amount of IL-6 in the stimulated condition was 3.20 ± 1.10 pg/mL. Cetirizine 0.1 μM was used as the reference compound; ** $p < 0.01$, *** $p < 0.001$ vs. stimulus.

These results suggest that RNLE might not counteract itching by inhibiting histamine signaling in keratinocytes. Nevertheless, several authors have reported that, in a wider scenario, flavonols and their glycosides may impact histamine release and humoral responses [57,58], thus proposing a potential antiallergic activity toward other cellular populations.

2.11. Quercetin and Kaempferol Preferentially Inhibit IFN- γ -Induced s-ICAM-1 Release in HaCaT Cells

At this point of our work, we wondered if the bioactivity of RNLE could be attributed to the main flavonoids detected in the extract. For this purpose, we selected quercetin and kaempferol (0.1–1 μ M) as representative pharmacophores of the parent glycosidic flavonols. Then, we treated HaCaT cells with the flavonols in the presence of TNF- α or IFN- γ to observe the effect on s-ICAM-1 release, thus allowing a reliable comparison with the experiments showed in Figure 7.

Quercetin and kaempferol preferentially inhibited IFN- γ -induced s-ICAM-1 release in a concentration-dependent fashion, thus resembling the activity of RNLE (Figure 14). Furthermore, their inhibitory concentration range was representative of that achievable by RNLE treatment, as evident from the quantitative analysis. However, kaempferol resulted more potent than quercetin against both stimulations with either TNF- α (IC_{50} = 0.77 and IC_{50} > 1 μ M, respectively) or IFN- γ (IC_{50} = 0.46 and IC_{50} > 1 μ M, respectively).

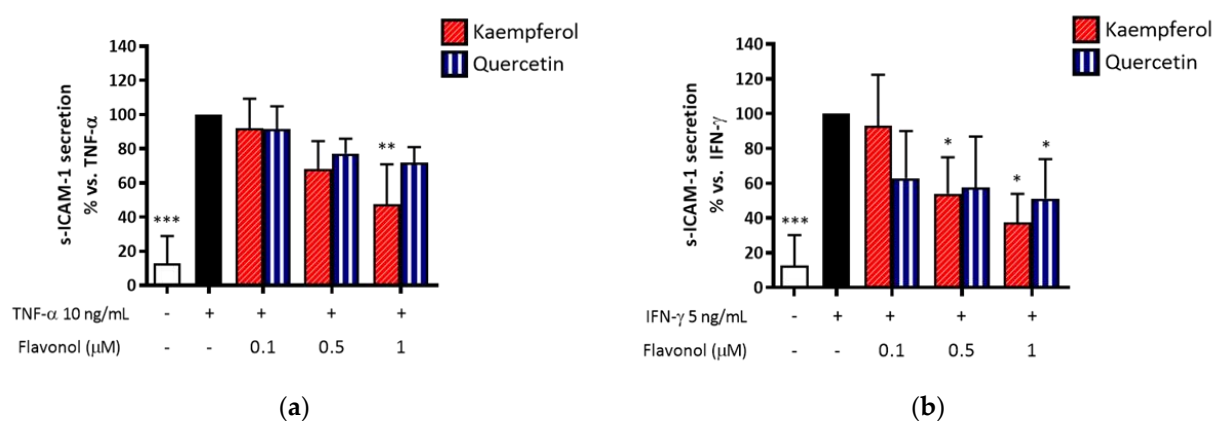


Figure 14. (a) Effect of quercetin and kaempferol treatment (0.1–1 μ M) on s-ICAM-1 release in HaCaT cells stimulated with TNF- α (10 ng/mL, 24 h). (b) Effect of quercetin and kaempferol treatment (0.1–1 μ M) on s-ICAM-1 release in HaCaT cells stimulated with IFN- γ (5 ng/mL, 24 h). * p < 0.05, ** p < 0.01, *** p < 0.001 vs. stimulus.

3. Conclusions

In the present work, a flavonol-rich blackcurrant leaf extract (RNLE) was discovered to preferentially counteract IFN- γ -mediated, rather than IL-4 mediated, inflammation in keratinocytes. RNLE strongly inhibited the release of IL-6 following TNF- α /IFN- γ , but not TNF- α /IL-4 challenge. The effect against IFN- γ challenge was also highlighted by the strong inhibition of IFN- γ -mediated s-ICAM-1 release, recognized as a marker of cell-mediated immunity in skin. This effect was attributed to the aglycones of the main flavonoids present in the extract: quercetin and kaempferol. Nevertheless, the extract was also able to inhibit TNF- α /IL-4-induced TSLP release, thus opening questions related to the potential impact on Th1/Th2 balance in inflammatory-based skin diseases.

Although the inhibition of NF- κ B activity explained, at least in part, the mechanism of action, our work demands further dermatological studies involving other potential molecular targets for flavonols, such as JAK/STAT and PKA signaling. The inhibition of IL-6 and TSLP release suggests an alternative antiallergic and antipruritic effect, which can add to the known antihistaminic effect of flavonols on skin cell populations other than keratinocytes. The findings of our study ascribe to *R. nigrum* leaf extract anti-inflammatory activities that could be exploited and may exert synergic effects in association with other blackcurrant products, such as seed oil, widely recognized for its promising beneficial effects at a cutaneous level due to the presence of γ -linolenic acid.

A deeper molecular investigation may clarify the role of blackcurrant leaf extracts in specific inflammatory disturbances, in which IFN- γ plays a central role, such as psoriasis and arthritis, one of the traditional indications reported in the ESCOP monograph.

4. Materials and Methods

Ribes nigrum leaf extract (RNLE) is a dry extract obtained from the extraction of *Ribes nigrum* L. leaves with aqueous solvent (extract to drug ratio 1:3). The extract was kindly provided by Drex Pharma S.r.l., via Privata Tarvisio, 32–20,125 Milano (MI) Italy.

4.1. Cell Culture

HaCaT (CVCL-0038; Cell Line Service, Eppelheim, Germany), a spontaneously immortalized human keratinocyte cell line from adult skin [59], was maintained at 37 °C, in a humidified atmosphere containing 5% CO₂, in Dulbecco's modified Eagle's medium (DMEM; Merck Life Science, Milano, Italy) supplemented with 10% heat-inactivated fetal bovine serum (Euroclone, Pero, Italy), 100 U/mL penicillin, 100 µg/mL streptomycin (Pen Strep Gibco™; Thermo Fisher Scientific, Monza, Italy), and 2 mM L-glutamine (Thermo Fisher Scientific, Monza, Italy). Every 4 days, cells were detached from 75 cm² flasks (Primo®; Euroclone, Pero, Italy) using Trypsin-EDTA 0.25% (Gibco™; Thermo Fisher Scientific, Monza, Italy), counted, and sub-cultured in a new flask or seeded in 24-well plates (Falcon®; Corning Life Sciences, Amsterdam, Netherlands) for the biological tests.

4.2. Cell Treatments

HaCaT were seeded at a density of 6×10^4 cells/well in 24-well flat-bottom multiwell plates (Falcon®; Corning Life Sciences, Amsterdam, Netherlands). After 72 h of growth, cells were treated with RNLE, alone, to assess cytotoxicity, or in the presence of different proinflammatory stimuli, i.e., human recombinant TNF-α (Peprotech, London, UK), alone or in combination with IFN-γ (PeproTech, London, UK), IL-4 (Peprotech, London, UK), or histamine (Merck Life Science, Milano, Italy). For the assessment of specific parameters, HaCaT cells were differentiated by maintaining HaCaT cells in multiwell plates under the previously stated cultural conditions over a period of 11 days for time course experiments [34,36]. In particular, differentiated cells were grown under high-calcium medium (DMEM, supplemented as stated in the previous section with the addition of Ca²⁺ 1.8 mM) for 9 days, replacing the medium every 48 h, and then treated for 24 h as mentioned below. The differentiation paradigm was previously validated by the assessment of cytokeratin-10 and involucrin protein synthesis (data not shown).

Depending on the biological parameter to be evaluated, the following specific treatment protocols were used:

- TNF-α 10 ng/mL, 6 h: assessment of gene expression; IL-8, IL-10, and s-ICAM-1 release; NF-κB-driven transcription.
- TNF-α 10 ng/mL, 24 h: assessment of s-ICAM-1 release.
- TNF-α 10 ng/mL + IFN-γ 5 ng/mL or IFN-γ 5 ng/mL, 24 h: assessment of IL-8, IL-6, and s-ICAM-1 release; NF-κB-driven transcription.
- TNF-α 25 ng/mL + histamine 100 µM or histamine 100 µM alone, 24 h: assessment of IL-6 release.
- TNF-α 20 ng/mL + IL-4 100 ng/mL, 24 h, differentiated cells: assessment of IL-6 and TSLP release; intracellular cAMP levels.
- TNF-α 20 ng/mL + IL-4 100 ng/mL, 6 h: assessment of NF-κB-driven transcription.

Crisaborole (Merck Life Science, Milano, Italy) 0.5 µM, cetirizine (Merck Life Science, Milano, Italy) 0.1 µM, (–)-epigallocatechin 3-gallate (EGCG) (PhytoLab, Vestenbergsgreuth, Germany) 20 µM, and apigenin (Sequoia Research Product, Pangbourne, UK) 20 µM were used as reference inhibitory compounds. EGCG was used in all the experiments involving NF-κB activation and the release of proinflammatory mediators [14], whereas crisaborole/apigenin and cetirizine were specifically used in experiments assessing cAMP and histamine contribution, respectively.

All treatments were performed using Dulbecco's modified Eagle's medium (DMEM; Merck Life Science, Milano, Italy) supplemented with 100 U/mL penicillin, 100 µg/mL streptomycin (Pen Strep Gibco™; Thermo Fisher Scientific, Monza, Italy) and 2 mM L-

glutamine (Thermo Fisher Scientific, Monza, Italy). At the end of the treatments, media or cell lysates were collected and stored at $-20\text{ }^{\circ}\text{C}$ until the subsequent biological assays.

4.3. Cytotoxicity and Viability Assays

The integrity of cellular morphology, before and after the treatment, was assessed by light microscopy.

4.3.1. Neutral Red Uptake (NRU) Assay

Cell viability was evaluated using the neutral red (3-amino-7-dimethylamino-2-methylphenazine hydrochloride; Merck Life Science, Milano, Italy) uptake assay, adapted from Repetto et al. [60]. After 24 h of incubation in presence of increasing concentrations of RNLE, the culture medium was substituted with 200 μL of neutral red medium (40 $\mu\text{g}/\text{mL}$), and cells were further incubated for 2 h at $37\text{ }^{\circ}\text{C}$. Then, medium was discarded, cells were thoroughly washed with PBS, and 200 μL of destaining solution (EtOH 50% *v/v* + 1% *v/v* glacial acetic acid) was added to each well. The plate was kept on a plate shaker for 10 min, 100 μL of medium was taken from each well and transferred to a 96-well plate, and the absorbance was measured with an EnVision Multimode Plate Reader (Perkin Elmer, Milano, Italy) at a wavelength of 535 nm.

4.3.2. LDH Assay

The potential cytotoxic effect of RNLE was determined in terms of release of lactate dehydrogenase (LDH) from cells into the extracellular medium using the LDH Cytotoxicity Detection Kit (Takara Bio Europe, Saint-Germain-en-Laye, France), following the manufacturer's instructions. To overcome the limitations due to the underestimation of the proportion of dead cells in conditions with growth inhibition, a modified protocol including additional condition-specific controls, consisting of the measurement of maximal LDH release for each individual treatment, was used [61]. After 24 h of incubation in presence of increasing concentrations of RNLE, Triton X-100 was added to condition-specific control wells (final concentration 1%) in order to obtain maximal LDH release, and the plate was centrifuged at $250\times g$ for 10 min. Then, 50 μL of supernatant was taken from each well, transferred to a 96-well plate, diluted with 50 μL of water, and mixed with 100 μL of reaction mixture. After 30 min of incubation at room temperature protected from light, the absorbance of the sample was measured with a VICTOR X3 Multilabel Plate Reader (Perkin Elmer, Milano, Italy) at a wavelength of 490 nm. Percentage cytotoxicity was calculated according to the equation proposed by Smith et al. [61].

The extract did not show any cytotoxic effect in the NRU assay in the range of tested concentrations (5–250 $\mu\text{g}/\text{mL}$). Absence of cytotoxicity was confirmed by lactate dehydrogenase (LDH) assay (Figures A1 and A2, Appendix A).

4.4. Phytochemical Characterization

4.4.1. Folin–Ciocâlțeu Assay

To assess the total phenolic content (TPC), RNLE was dissolved in water (5 mg/mL) and 20 μL was diluted to a final volume of 800 μL , equivalent to 100 μg of extract. Then, 50 μL of 2 N Folin–Ciocâlțeu reagent (Merck Life Science, Milano, Italy) and 150 μL of 20% (*w/v*) Na_2CO_3 were added. After 30 min of incubation at $37\text{ }^{\circ}\text{C}$, samples were transferred to plastic cuvettes, and absorbance was measured with a Jasco V630 Spectrophotometer at a wavelength of 765 nm against a gallic acid calibration curve.

4.4.2. Mass Spectrometry

Qualitative and quantitative analyses were carried out by LC–MS/MS using a LC system Surveyor MS PUMP PLUS (Thermo Fisher Scientific, Monza, Italy) coupled with an LTQ ion-trap mass spectrometer (Thermo Fisher Scientific, Monza, Italy) equipped with an ESI source operating in the negative mode. The column used was a XSelect HSS T3 XP (100 \AA , 2.5 μm , $2.1\times 100\text{ mm}$; Waters, Sesto San Giovanni, Italy) with a flow rate of

0.15 mL/min. A gradient elution was performed, and the mobile phase was a mixture of water containing 0.1% formic acid (A) and acetonitrile (B). The elution gradient was set as follows: 0–1 min (5% B), 1–10 min (5–100% B), 10–15 min (100% B), 15–25 min (100–5% B). The operating conditions for MS analysis were as follows: spray voltage, -5 kV; capillary temperature, 250 °C; sheath gas and auxiliary gas flow, 60 and 5 arbitrary units, respectively; tube lens, -110 V; total ion current (TIC); base peak-dependent mass range, m/z 230–1500; collision energy, 20 eV.

Compounds in the extract (injection: 25 μ g) were identified by comparison of the retention times and mass spectra with those of authentic compounds (injection: 5 or 10 ng) commercially available at a high grade of purity.

4.5. Gene Expression Analysis

4.5.1. RNA Extraction

At the end of the 6 h treatment, the medium was removed, and the cells were washed with PBS and lysed with QIAzol Lysis Reagent (QIAGEN GmbH, Hilden, Germany) according to the manufacturer's instructions. The lysates were homogenized and kept frozen until the following RNA purification steps. Total RNA was isolated from cell lysates with miRNeasy Mini Kit (QIAGEN, Hilden, Germany), according to the manufacturer's protocol. A set of RNase-free DNase (QIAGEN, Hilden, Germany) was used to provide efficient on-column digestion of genomic DNA. Total RNA was eluted with 35 μ L of nuclease-free water. The concentration and quality of the purified RNA were assessed spectrophotometrically using a NanoDrop ND-1000 spectrophotometer (Thermo Fisher Scientific, Monza, Italy). Sample purity was estimated by measuring A260/280 and A260/230 ratios of spectrophotometric absorbance to check for possible copurified contaminants during the RNA isolation.

4.5.2. cDNA Synthesis

Residual genomic DNA elimination and cDNA synthesis were performed with the RT² First Strand Kit (QIAGEN, Hilden, Germany), according to the manufacturer's indications, using 400 ng of total RNA for each sample.

4.5.3. qPCR

The analysis of gene expression was performed using a 384-well PCR array related to human genes involved in wound healing (RT² Profiler PCR Array PAHS-121Z Human Wound Healing; QIAGEN, Hilden, Germany). Each well of the array contained different primers for a specific target gene (in total 84 different target genes) or housekeeping gene for data normalization. Control wells were present to assess genomic DNA contamination, as well as the quality of the reverse transcription and PCR reactions. A quantity of cDNA equivalent to 400 ng of total RNA was mixed with SYBR[®] Green Master Mix RT² Reagent (QIAGEN, Hilden, Germany) according to the manufacturer's instructions and aliquoted into the 384-well array. The real-time qPCR was performed using a CFX384[™] Real-Time PCR Detection System (Bio-Rad Laboratories, Segrate, Italy). The threshold cycle value for each gene (C_t) was automatically provided by software CFX Manager[™] (Bio-Rad Laboratories, Segrate, Italy), depending on the amplification curves, and the threshold was manually set as recommended by the RT² Profiler PCR Array manual. The C_t cut-off was set to 35. Expression data were normalized to the housekeeping gene RPLP0 (ribosomal protein lateral stalk subunit P0) and elaborated using the $\Delta\Delta C_t$ method based on Pfaffl equation [62].

4.6. NF- κ B-Driven Transcription

HaCaT cells were transiently transfected with a reporter NF- κ B-Luc plasmid (250 ng per well), containing the luciferase gene under the control of the E-selectin promoter characterized by three κ B responsive elements, using Lipofectamine[®] 3000 Transfection Reagent (Invitrogen[®]; Thermo Fisher Scientific, Monza, Italy). The plasmid NF- κ B-Luc

was a gift from Dr. N. Marx (Department of Internal Medicine-Cardiology, University of Ulm; Ulm, Germany). Sixteen hours later, cells were treated as previously stated. At the end of the treatment, the amount of luciferase produced into the cells was assessed using Britelite™ Plus reagent (Perkin Elmer, Milano, Italy) according to the manufacturer's instructions. The luminescence deriving from the reaction between luciferase and luciferin was measured with a VICTOR X3 Multilabel Plate Reader (Perkin Elmer, Milano, Italy). The results (mean \pm SD of at least three experiments) were expressed as percentage relative to stimulated control, which was arbitrarily assigned the value of 100%.

4.7. Measurement of IL-6, IL-8, IL-10, TSLP, and s-ICAM-1 Release

The release of IL-6, IL-8, IL-10, TSLP, and s-ICAM-1 was evaluated by enzyme-linked immunosorbent assay (ELISA) on culture media. The amount of intracellular IL-10 was assayed in whole-cell lysates obtained with a buffer containing 150 mM NaCl, 1% IGEPAL® CA-630, and 50 mM Tris pH 8.0 supplemented with protease inhibitor cocktail (all from Merck Life Science, Milano, Italy). Sample loading was normalized according to the protein content, determined with the BCA method (Quantum Protein Assay Kit; Euroclone, Pero, Italy).

Human IL-6, IL-8, IL-10, TSLP, and ICAM-1 ELISA development kits were purchased from PeproTech (PeproTech, London, UK). Corning 96-well EIA/RIA plates (Merck Life Science, Milano, Italy) were coated overnight at room temperature with the capture antibody contained in the kit. The amounts of IL-6, IL-8, IL-10, TSLP, and s-ICAM-1 in the samples were detected by measuring the absorbance resulted from the colorimetric reaction between horseradish peroxidase enzyme and 2,2'-azino-bis(3-ethylbenzothiazoline-6-sulfonic acid) (ABTS) or 3,3',5,5'-tetramethylbenzidine (TMB) substrate (Merck Life Science, Italy), according to the manufacturer's instructions. The signal was read using a spectrophotometer (VICTOR X3; PerkinElmer, Milano, Italy) at 405 nm (ABTS) or 450 nm (TMB). IL-6, IL-8, IL-10, TSLP, and s-ICAM-1 levels were quantified through a standard curve supplied with the ELISA kit. The results (mean \pm SD of at least three experiments) were expressed as percentage relative to stimulated control, which was arbitrarily assigned the value of 100%.

Preliminary time course experiments were performed to set the optimal experimental conditions for the subsequent experiments (see Appendix A).

4.8. Measurement of Intracellular cAMP Levels

After 9 days of differentiation, HaCaT cells were incubated for 24 h in presence of increasing concentrations of RNLE. At the end of the treatment, adherent cells were lysed with 100 μ L/well of 0.1 M hydrochloric acid at RT for 20 min. Samples were collected using a scraper and subjected to centrifugation at 1000 \times g for 10 min. The supernatant was transferred into new tubes, and total protein content was evaluated by BCA method. Samples (50 μ g of total proteins each) were diluted 1:2 with assay buffer and directly used for the evaluation of intracellular cAMP levels by a cyclic AMP ELISA kit (Cayman Chemical, Ann Arbor, MI, USA) according to the manufacturer's protocol. Absorbance of samples was measured with a VICTOR X3 Multilabel Plate Reader (Perkin Elmer, Milano, Italy) at a wavelength of 405 nm.

4.9. Statistical Analysis

All data were expressed as the mean \pm SD of at least three independent experiments. Gene expression results were calculated using the $\Delta\Delta C_t$ method. $\Delta\Delta C_t$ (\log_2 fold change) values were analyzed by multiple unpaired *t*-tests. ELISA assays were analyzed by unpaired one-way analysis of variance (ANOVA), followed by Bonferroni post hoc test.

Statistical analyses were performed using GraphPad Prism 8.0 software (GraphPad Software Inc., San Diego, CA, USA). Values of $p < 0.05$ were considered statistically significant.

Author Contributions: Conceptualization, M.D.; methodology, A.M., S.P., M.F. and G.M.; data curation, M.D. and E.S.; investigation, A.M., S.P. and F.G.; writing—original draft preparation, S.P. and A.M.; writing—review and editing, S.P., A.M., A.C., E.S. and M.D. All authors have read and agreed to the published version of the manuscript.

Funding: The present work was partially funded by Drex Pharma S.r.l., via Privata Tarvisio, 32—20125 Milano (MI) Italy. This research was supported by grants from MIUR “Progetto Eccellenza”.

Data Availability Statement: The data presented in this study are available on request from the corresponding author.

Acknowledgments: The authors thank Petra Boukamp and Norbert Fusenig from Deutsches Krebsforschungszentrum, Stiftung des öffentlichen Rechts (German Cancer Research Center, Heidelberg, Germany), Im Neuenheimer Feld 280, D-69120 Heidelberg, Germany, for providing the HaCaT cell line.

Conflicts of Interest: The authors declare no conflict of interest. A. Cammisa, M.D. is involved in the Medical and R&D area of Drex Pharma s.r.l., Milan, Italy, a pharmaceutical company that commercializes food supplements containing *Ribes nigrum* extracts. However, the funders had no role in the design of the study, collection, analyses, or interpretation of data; in the writing of the manuscript, or in the decision to publish the results. This paper does not necessarily reflect Drex Pharma’s views of its future policy on this area.

Appendix A

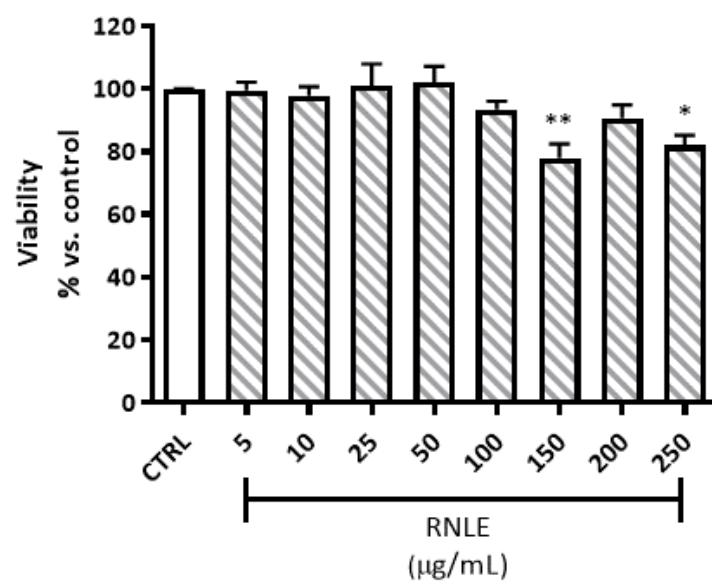


Figure A1. Effect of 24 h RNLE treatment (5–250 µg/mL) on HaCaT cell viability, as measured with Neutral Red Uptake (NRU) assay; * $p < 0.05$, ** $p < 0.01$ vs. stimulus.

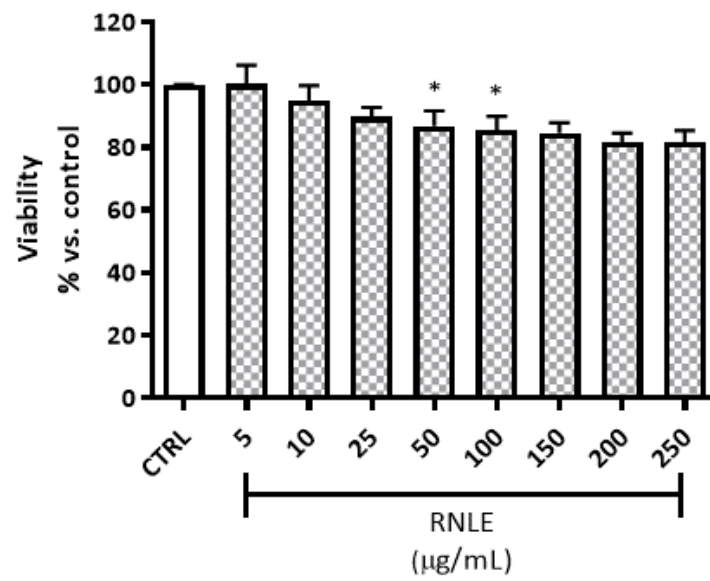


Figure A2. Effect of 24 h RNLE treatment (5–250 µg/mL) on HaCaT cell viability, as measured with LDH assay; * $p < 0.05$ vs. stimulus.

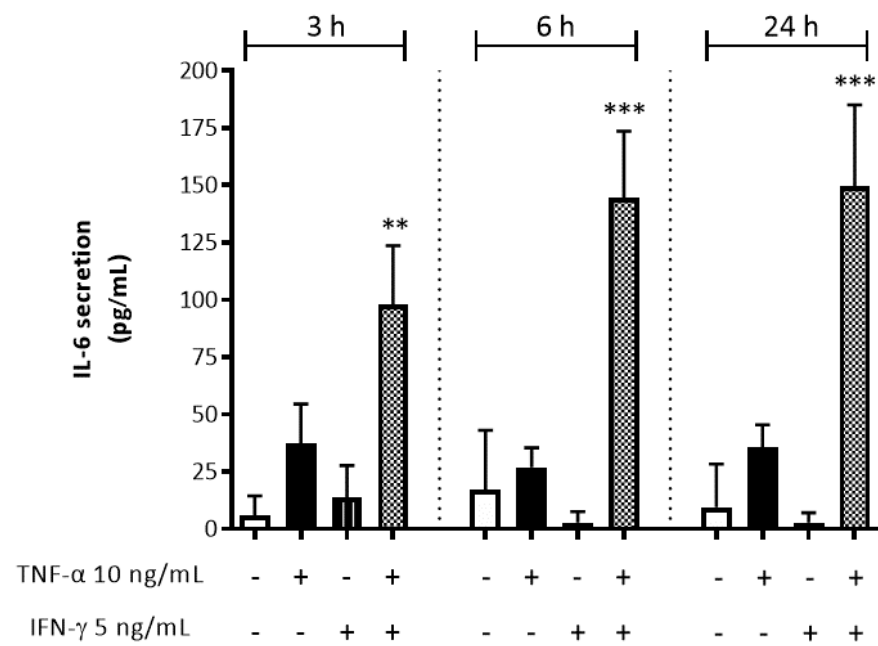


Figure A3. Preliminary time course experiment aimed at assessing IL-6 release from HaCaT cells stimulated with TNF-α (10 ng/mL), IFN-γ (5 ng/mL), or a combination of both; ** $p < 0.01$, *** $p < 0.001$ vs. stimulus.

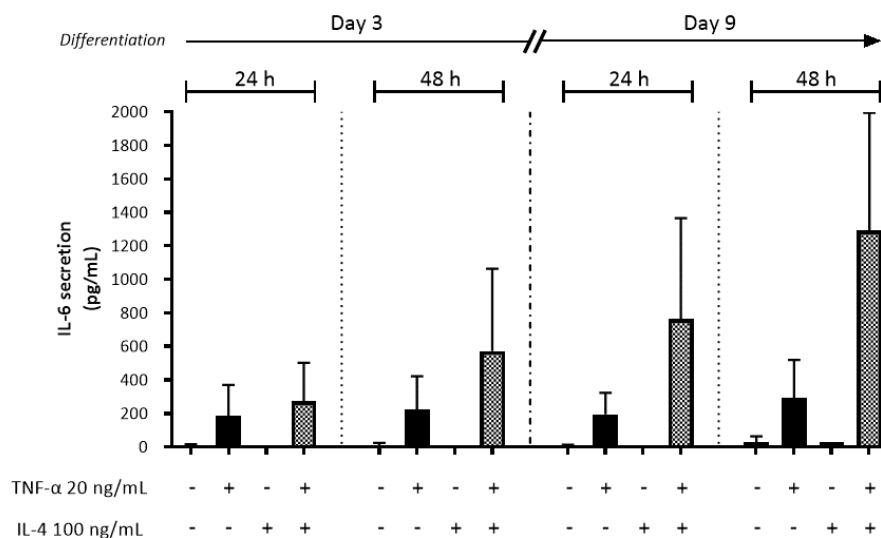


Figure A4. Preliminary time course experiment aimed at assessing IL-6 release from HaCaT cells at different stages of differentiation, stimulated with TNF- α (20 ng/mL), IL-4 (100 ng/mL), or a combination of both.

References

- Piazza, S.; Fumagalli, M.; Khalilpour, S.; Martinelli, G.; Magnavacca, A.; Dell'Agli, M.; Sangiovanni, E. A Review of the Potential Benefits of Plants Producing Berries in Skin Disorders. *Antioxid. Basel* **2020**, *9*, 542. [CrossRef] [PubMed]
- Committee on Herbal Medicinal Products (HMPC), European Union Herbal Monograph on *Ribes Nigrum* L. Folium. Available online: [EMA/HMPC/745353/2016](https://www.ema.europa.eu/en/medicines/human/EPAR/ribes-nigrum/ribes-nigrum.htm) (accessed on 1 April 2021).
- European Scientific Cooperative on Phytotherapy, ESCOP Monographs, The Scientific Foundation for Herbal Medicinal Products. *Ribes Nigri Folium (Black Currant Leaf)*; Online Series; ESCOP: Exeter, UK, 2017.
- Liu, P.; Kallio, H.; Yang, B. Flavonol glycosides and other phenolic compounds in buds and leaves of different varieties of black currant (*Ribes nigrum* L.) and changes during growing season. *Food Chem.* **2014**, *160*, 180–189. [CrossRef]
- Tabart, J.; Kevers, C.; Evers, D.; Dommes, J. Ascorbic acid, phenolic acid, flavonoid, and carotenoid profiles of selected extracts from *Ribes nigrum*. *J. Agric. Food Chem.* **2011**, *59*, 4763–4770. [CrossRef]
- Garbacki, N.; Kinet, M.; Nusgens, B.; Desmecht, D.; Damas, J. Proanthocyanidins, from *Ribes nigrum* leaves, reduce endothelial adhesion molecules ICAM-1 and VCAM-1. *J. Inflamm. (Lond.)* **2005**, *2*, 9. [CrossRef] [PubMed]
- Mongold, J.J.; Susplugas, P.; Taillade, C.; Serrano, J.J. Anti-inflammatory activity of *Ribes nigrum* leaf extract in rats. *Plantes Méd. Phytothér.* **1993**, *26*, 109–116.
- Kendir, G.; Sutar, I.; Ceribasi, A.O.; Koroglu, A. Activity evaluation on *Ribes* species, traditionally used to speed up healing of wounds: With special focus on *Ribes nigrum*. *J. Ethnopharmacol.* **2019**, *237*, 141–148. [CrossRef]
- Jung, J.W.; Kim, S.J.; Ahn, E.M.; Oh, S.R.; Lee, H.J.; Jeong, J.A.; Lee, J.Y. *Ribes fasciculatum* var. *chinense* Attenuated Allergic Inflammation In Vivo and In Vitro. *Biomol. Ther. (Seoul)* **2014**, *22*, 547–552. [CrossRef]
- Kim, J.E.; Kim, J.S.; Cho, D.H.; Park, H.J. Molecular Mechanisms of Cutaneous Inflammatory Disorder: Atopic Dermatitis. *Int. J. Mol. Sci.* **2016**, *17*, 1234. [CrossRef]
- Girolomoni, G.; Strohal, R.; Puig, L.; Bachelez, H.; Barker, J.; Boehncke, W.H.; Prinz, J.C. The role of IL-23 and the IL-23/TH 17 immune axis in the pathogenesis and treatment of psoriasis. *J. Eur. Acad. Dermatol. Venereol.* **2017**, *31*, 1616–1626. [CrossRef]
- Lande, R.; Botti, E.; Jandus, C.; Dojcinovic, D.; Fanelli, G.; Conrad, C.; Chamilos, G.; Feldmeyer, L.; Marinari, B.; Chon, S.; et al. The antimicrobial peptide LL37 is a T-cell autoantigen in psoriasis. *Nat. Commun.* **2014**, *5*, 5621. [CrossRef] [PubMed]
- Corren, J.; Ziegler, S.F. TSLP: From allergy to cancer. *Nat. Immunol.* **2019**, *20*, 1603–1609. [CrossRef] [PubMed]
- Sangiovanni, E.; Fumagalli, M.; Pacchetti, B.; Piazza, S.; Magnavacca, A.; Khalilpour, S.; Melzi, G.; Martinelli, G.; Dell'Agli, M. Cannabis sativa L. extract and cannabidiol inhibit in vitro mediators of skin inflammation and wound injury. *Phytother. Res.* **2019**, *33*, 2083–2093. [CrossRef] [PubMed]
- Johnston, A.; Fritz, Y.; Dawes, S.M.; Diaconu, D.; Al-Attar, P.M.; Guzman, A.M.; Chen, C.S.; Fu, W.; Gudjonsson, J.E.; McCormick, T.S.; et al. Keratinocyte overexpression of IL-17C promotes psoriasiform skin inflammation. *J. Immunol.* **2013**, *190*, 2252–2262. [CrossRef] [PubMed]
- Albanesi, C.; Cavani, A.; Girolomoni, G. IL-17 is produced by nickel-specific T lymphocytes and regulates ICAM-1 expression and chemokine production in human keratinocytes: Synergistic or antagonist effects with IFN- γ and TNF- α . *J. Immunol.* **1999**, *162*, 494–502.

17. El Darzi, E.; Bazzi, S.; Daoud, S.; Echtay, K.S.; Bahr, G.M. Differential regulation of surface receptor expression, proliferation, and apoptosis in HaCaT cells stimulated with interferon-gamma, interleukin-4, tumor necrosis factor-alpha, or muramyl dipeptide. *Int. J. Immunopathol. Pharmacol.* **2017**, *30*, 130–145. [CrossRef] [PubMed]
18. Derocq, J.M.; Segui, M.; Poinot-Chazel, C.; Minty, A.; Caput, D.; Ferrara, P.; Casellas, P. Interleukin-13 stimulates interleukin-6 production by human keratinocytes. Similarity with interleukin-4. *FEBS Lett.* **1994**, *343*, 32–36. [CrossRef]
19. Kohda, F.; Koga, T.; Uchi, H.; Urabe, K.; Furue, M. Histamine-induced IL-6 and IL-8 production are differentially modulated by IFN-gamma and IL-4 in human keratinocytes. *J. Dermatol. Sci.* **2002**, *28*, 34–41. [CrossRef]
20. Hirano, T. Interleukin 6 and its receptor: Ten years later. *Int. Rev. Immunol.* **1998**, *16*, 249–284. [CrossRef] [PubMed]
21. Yuk, C.M.; Park, H.J.; Kwon, B.I.; Lah, S.J.; Chang, J.; Kim, J.Y.; Lee, K.M.; Park, S.H.; Hong, S.; Lee, S.H. Basophil-derived IL-6 regulates TH17 cell differentiation and CD4 T cell immunity. *Sci. Rep.* **2017**, *7*, 41744. [CrossRef] [PubMed]
22. Kim, H.J.; Baek, J.; Lee, J.R.; Roh, J.Y.; Jung, Y. Optimization of Cytokine Milieu to Reproduce Atopic Dermatitis-related Gene Expression in HaCaT Keratinocyte Cell Line. *Immune Netw.* **2018**, *18*, e9. [CrossRef]
23. Cortez, R.E.; Gonzalez de Mejia, E. Blackcurrants (Ribes nigrum): A Review on Chemistry, Processing, and Health Benefits. *J. Food Sci.* **2019**, *84*, 2387–2401. [CrossRef] [PubMed]
24. Boston University—Gene Resources NF-κB Target Genes. Available online: <http://www.bu.edu/nf-kb/gene-resources/target-genes/> (accessed on 10 April 2021).
25. Satoh, J.; Tabunoki, H. A Comprehensive Profile of ChIP-Seq-Based STAT1 Target Genes Suggests the Complexity of STAT1-Mediated Gene Regulatory Mechanisms. *Gene Regul. Syst. Biol.* **2013**, *7*, 41–56. [CrossRef] [PubMed]
26. Kanda, N.; Shimizu, T.; Tada, Y.; Watanabe, S. IL-18 enhances IFN-gamma-induced production of CXCL9, CXCL10, and CXCL11 in human keratinocytes. *Eur. J. Immunol.* **2007**, *37*, 338–350. [CrossRef]
27. Park, J.H.; Kim, M.S.; Jeong, G.S.; Yoon, J. Xanthii fructus extract inhibits TNF-alpha/IFN-gamma-induced Th2-chemokines production via blockade of NF-kappaB, STAT1 and p38-MAPK activation in human epidermal keratinocytes. *J. Ethnopharmacol.* **2015**, *171*, 85–93. [CrossRef] [PubMed]
28. Kjaergaard, A.G.; Dige, A.; Krog, J.; Tonnesen, E.; Wogensen, L. Soluble adhesion molecules correlate with surface expression in an in vitro model of endothelial activation. *Basic Clin. Pharmacol. Toxicol.* **2013**, *113*, 273–279. [CrossRef] [PubMed]
29. Collins, T.; Read, M.A.; Neish, A.S.; Whitley, M.Z.; Thanos, D.; Maniatis, T. Transcriptional regulation of endothelial cell adhesion molecules: NF-kappa B and cytokine-inducible enhancers. *FASEB J.* **1995**, *9*, 899–909. [CrossRef]
30. Lee, W.; Ku, S.K.; Bae, J.S. Barrier protective effects of rutin in LPS-induced inflammation in vitro and in vivo. *Food Chem. Toxicol.* **2012**, *50*, 3048–3055. [CrossRef]
31. Li, C.; Zhang, W.J.; Frei, B. Quercetin inhibits LPS-induced adhesion molecule expression and oxidant production in human aortic endothelial cells by p38-mediated Nrf2 activation and antioxidant enzyme induction. *Redox Biol.* **2016**, *9*, 104–113. [CrossRef]
32. Bito, T.; Roy, S.; Sen, C.K.; Shirakawa, T.; Gotoh, A.; Ueda, M.; Ichihashi, M.; Packer, L. Flavonoids differentially regulate IFN gamma-induced ICAM-1 expression in human keratinocytes: Molecular mechanisms of action. *FEBS Lett.* **2002**, *520*, 145–152. [CrossRef]
33. Son, E.D.; Kim, H.J.; Kim, K.H.; Bin, B.H.; Bae, I.H.; Lim, K.M.; Yu, S.J.; Cho, E.G.; Lee, T.R. S100A7 (psoriasin) inhibits human epidermal differentiation by enhanced IL-6 secretion through IκB/NF-κB signalling. *Exp. Dermatol.* **2016**, *25*, 636–641. [CrossRef]
34. Omori-Miyake, M.; Yamashita, M.; Tsunemi, Y.; Kawashima, M.; Yagi, J. In vitro assessment of IL-4- or IL-13-mediated changes in the structural components of keratinocytes in mice and humans. *J. Invest. Dermatol.* **2014**, *134*, 1342–1350. [CrossRef] [PubMed]
35. Bao, L.; Alexander, J.B.; Zhang, H.; Shen, K.; Chan, L.S. Interleukin-4 Downregulation of Involucrin Expression in Human Epidermal Keratinocytes Involves Stat6 Sequestration of the Coactivator CREB-Binding Protein. *J. Interferon Cytokine Res.* **2016**, *36*, 374–381. [CrossRef] [PubMed]
36. Colombo, I.; Sangiovanni, E.; Maggio, R.; Mattozzi, C.; Zava, S.; Corbett, Y.; Fumagalli, M.; Carlino, C.; Corsetto, P.A.; Scacabarozzi, D.; et al. HaCaT Cells as a Reliable In Vitro Differentiation Model to Dissect the Inflammatory/Repair Response of Human Keratinocytes. *Mediat. Inflamm.* **2017**, *2017*, 7435621. [CrossRef] [PubMed]
37. Nishio, H.; Matsui, K.; Tsuji, H.; Tamura, A.; Suzuki, K. Immunolocalisation of the janus kinases (JAK)—Signal transducers and activators of transcription (STAT) pathway in human epidermis. *J. Anat.* **2001**, *198*, 581–589. [CrossRef]
38. Bogiatzi, S.I.; Fernandez, I.; Bichet, J.C.; Marloie-Provost, M.A.; Volpe, E.; Sastre, X.; Soumelis, V. Cutting Edge: Proinflammatory and Th2 cytokines synergize to induce thymic stromal lymphopoietin production by human skin keratinocytes. *J. Immunol.* **2007**, *178*, 3373–3377. [CrossRef]
39. Divekar, R.; Kita, H. Recent advances in epithelium-derived cytokines (IL-33, IL-25, and thymic stromal lymphopoietin) and allergic inflammation. *Curr. Opin. Allergy Clin. Immunol.* **2015**, *15*, 98–103. [CrossRef]
40. Zhang, X.; Pathak, T.; Yoast, R.; Emrich, S.; Xin, P.; Nwokonko, R.M.; Johnson, M.; Wu, S.; Delierneux, C.; Gueguinou, M.; et al. A calcium/cAMP signaling loop at the ORAI1 mouth drives channel inactivation to shape NFAT induction. *Nat. Commun.* **2019**, *10*, 1971. [CrossRef]
41. Vu, A.T.; Chen, X.; Xie, Y.; Kamijo, S.; Ushio, H.; Kawasaki, J.; Hara, M.; Ikeda, S.; Okumura, K.; Ogawa, H.; et al. Extracellular double-stranded RNA induces TSLP via an endosomal acidification- and NF-kappaB-dependent pathway in human keratinocytes. *J. Invest. Dermatol.* **2011**, *131*, 2205–2212. [CrossRef]

42. Parry, G.C.; Mackman, N. Role of cyclic AMP response element-binding protein in cyclic AMP inhibition of NF-kappaB-mediated transcription. *J. Immunol.* **1997**, *159*, 5450–5456.
43. Dong, C.; Virtucio, C.; Zemska, O.; Baltazar, G.; Zhou, Y.; Baia, D.; Jones-Iatauro, S.; Sexton, H.; Martin, S.; Dee, J.; et al. Treatment of Skin Inflammation with Benzoxaborole Phosphodiesterase Inhibitors: Selectivity, Cellular Activity, and Effect on Cytokines Associated with Skin Inflammation and Skin Architecture Changes. *J. Pharmacol. Exp. Ther.* **2016**, *358*, 413–422. [[CrossRef](#)]
44. Mammone, T.; Marenus, K.; Maes, D.; Lockshin, R.A. The induction of terminal differentiation markers by the cAMP pathway in human HaCaT keratinocytes. *Skin Pharmacol. Appl. Skin Physiol.* **1998**, *11*, 152–160. [[CrossRef](#)]
45. Dell’Agli, M.; Galli, G.V.; Bosisio, E. Inhibition of cGMP-phosphodiesterase-5 by biflavones of Ginkgo biloba. *Planta Med.* **2006**, *72*, 468–470. [[CrossRef](#)]
46. Ko, W.C.; Shih, C.M.; Lai, Y.H.; Chen, J.H.; Huang, H.L. Inhibitory effects of flavonoids on phosphodiesterase isozymes from guinea pig and their structure-activity relationships. *Biochem. Pharmacol.* **2004**, *68*, 2087–2094. [[CrossRef](#)]
47. Chaabi, M.; Antheaume, C.; Weniger, B.; Justiniano, H.; Lugnier, C.; Lobstein, A. Biflavones of Decussocarpus rospigliosii as phosphodiesterases inhibitors. *Planta Med.* **2007**, *73*, 1284–1286. [[CrossRef](#)] [[PubMed](#)]
48. Jegal, J.; Park, N.J.; Park, S.A.; Bong, S.K.; Jegal, H.; Kim, S.N.; Yang, M.H. Juniperus chinensis Fruits Attenuate Oxazolone- and 2,4-Dinitrochlorobenzene-Induced Atopic Dermatitis Symptoms in Mice. *Biol. Pharm. Bull.* **2018**, *41*, 259–265. [[CrossRef](#)]
49. Park, C.H.; Min, S.Y.; Yu, H.W.; Kim, K.; Kim, S.; Lee, H.J.; Kim, J.H.; Park, Y.J. Effects of Apigenin on RBL-2H3, RAW264.7, and HaCaT Cells: Anti-Allergic, Anti-Inflammatory, and Skin-Protective Activities. *Int. J. Mol. Sci.* **2020**, *21*, 4620. [[CrossRef](#)] [[PubMed](#)]
50. Murray, A.J. Pharmacological PKA inhibition: All may not be what it seems. *Sci. Signal.* **2008**, *1*, re4. [[CrossRef](#)] [[PubMed](#)]
51. Woo, T.E.; Kuzel, P. Crisaborole 2% Ointment (Eucrisa) for Atopic Dermatitis. *Skin Ther. Lett.* **2019**, *24*, 4–6.
52. Beekmann, K.; de Haan, L.H.; Actis-Goretta, L.; van Bladeren, P.J.; Rietjens, I.M. Effect of Glucuronidation on the Potential of Kaempferol to Inhibit Serine/Threonine Protein Kinases. *J. Agric. Food Chem.* **2016**, *64*, 1256–1263. [[CrossRef](#)]
53. Wang, X.F.; Song, S.D.; Li, Y.J.; Hu, Z.Q.; Zhang, Z.W.; Yan, C.G.; Li, Z.G.; Tang, H.F. Protective Effect of Quercetin in LPS-Induced Murine Acute Lung Injury Mediated by cAMP-Epac Pathway. *Inflammation* **2018**, *41*, 1093–1103. [[CrossRef](#)]
54. Brenner, S.; Prosch, S.; Schenke-Layland, K.; Riese, U.; Gausmann, U.; Platzer, C. cAMP-induced Interleukin-10 promoter activation depends on CCAAT/enhancer-binding protein expression and monocytic differentiation. *J. Biol. Chem.* **2003**, *278*, 5597–5604. [[CrossRef](#)] [[PubMed](#)]
55. Wilson, S.R.; The, L.; Batia, L.M.; Beattie, K.; Katibah, G.E.; McClain, S.P.; Pellegrino, M.; Estandian, D.M.; Bautista, D.M. The epithelial cell-derived atopic dermatitis cytokine TSLP activates neurons to induce itch. *Cell* **2013**, *155*, 285–295. [[CrossRef](#)] [[PubMed](#)]
56. Wolfle, U.; Haarhaus, B.; Schempp, C.M. Amarogentin Displays Immunomodulatory Effects in Human Mast Cells and Keratinocytes. *Mediat. Inflamm.* **2015**, *2015*, 630128. [[CrossRef](#)] [[PubMed](#)]
57. Mlcek, J.; Jurikova, T.; Skrovankova, S.; Sochor, J. Quercetin and Its Anti-Allergic Immune Response. *Molecules* **2016**, *21*, 623. [[CrossRef](#)]
58. Ganeshpurkar, A.; Saluja, A.K. Protective effect of rutin on humoral and cell mediated immunity in rat model. *Chem. Biol. Interact.* **2017**, *273*, 154–159. [[CrossRef](#)] [[PubMed](#)]
59. Boukamp, P.; Petrussevska, R.T.; Breitkreutz, D.; Hornung, J.; Markham, A.; Fusenig, N.E. Normal keratinization in a spontaneously immortalized aneuploid human keratinocyte cell line. *J. Cell Biol.* **1988**, *106*, 761–771. [[CrossRef](#)] [[PubMed](#)]
60. Repetto, G.; del Peso, A.; Zurita, J.L. Neutral red uptake assay for the estimation of cell viability/cytotoxicity. *Nat. Protoc.* **2008**, *3*, 1125–1131. [[CrossRef](#)]
61. Smith, S.M.; Wunder, M.B.; Norris, D.A.; Shellman, Y.G. A simple protocol for using a LDH-based cytotoxicity assay to assess the effects of death and growth inhibition at the same time. *PLoS ONE* **2011**, *6*, e26908. [[CrossRef](#)] [[PubMed](#)]
62. D’Alessandro, S.; Magnavacca, A.; Perego, F.; Fumagalli, M.; Sangiovanni, E.; Prato, M.; Dell’Agli, M.; Basilico, N. Effect of Hypoxia on Gene Expression in Cell Populations Involved in Wound Healing. *Biomed. Res. Int.* **2019**, *2019*, 2626374. [[CrossRef](#)]